SPATIAL DISTRIBUTION AND SEASONAL CHANGES OF URBAN AND SUBURBAN SURFACE RADIATION BUDGET IN BEIJING

J. Zhou, Y. H. Chen*, J. Li

State Key Laboratory of Earth Surface Processes and Resource Ecology, College of Resources Science & Technology, Beijing Normal University, Beijing 100875, China – (zhouji, cyh, lijing)@ires.cn

KEY WORDS: Albedo, Land Surface Temperature, Radiation Budget, Land Cover, Remote Sensing, Urban

ABSTRACT:

Under the context of rapid urbanization, radiation budget is crucial to analyse the adverse climate effects in urban environments, especially for mega-cities. Selected Beijing city and surrounding regions as the study area, this paper investigated the spatial distribution patterns and temporal variations of radiation budget based on integration of remote sensing images and ancillary data. Landsat-5 Thematic Mapper (TM) images and meteorological data acquired in the summer and winter were used to calculate land surface parameters and the net radiation flux. Validation with *in situ* measurement shows that the calculation of net radiation yielded high accuracy. In order to understand the spatial patterns of radiation budgets, the net radiation flux, albedo, and land surface temperature were analysed in terms of variations among different land cover types. Results indicate that the city can be characterized as a "basin" of net radiation in the summer, while a "plateau" in the winter. The albedo and land surface temperature were two primary factors contributing to the spatial variations of net radiation, while the solar elevation angle controlled the seasonal variations of the absolute amount.

1. INTRODUCTION

Fast urbanization induces adverse climatic effects for urban environments and surrounding areas, even for local and macro scale regions. Radiation budget, which is also named as net radiation flux and defined as the difference between the incoming and outgoing radiation fluxes at the surface of earth (Bisht *et al.*, 2005), plays as the dominant element of energy exchange between land surface and atmosphere. Because of intense human activities and complicated artificial landscapes, the radiation budget in urban environment is different from that of natural surfaces greatly. This has become one of the focuses of urban environment researches.

With the advent of satellite remote sensing, especially the remote sensors with higher spatial resolution at thermal channels, e. g. Landsat TM/ETM+, Terra ASTER, some researchers have examined the applicability and feasibility of these images to investigate the radiation budget in the urban and suburban areas (Chrysoulakis, 2003; Frey *et al.*, 2007; Rigo & Parlow, 2007). It has been confirmed that the integration of remote sensing images and ancillary data is an appropriate and helpful route to grasp the patterns of radiation budget in different urban areas and at different spatial and temporal scales.

As the capital and second largest city in China, Beijing has been influenced by intense urban climate problems because of its mass population, traffics and the unique physical settings. This paper has two objectives: 1) Calculation the net radiation flux of the urban and suburban areas in Beijing; 2) Analysis the spatial distribution patterns and seasonal changes of radiation budget. The results will be useful for understanding the change rules of urbanization in the process of urban climate for such a mega-city.

2. STUDY AREA AND DATA

Beijing city and surrounding regions were selected as the study area (Fig.1).

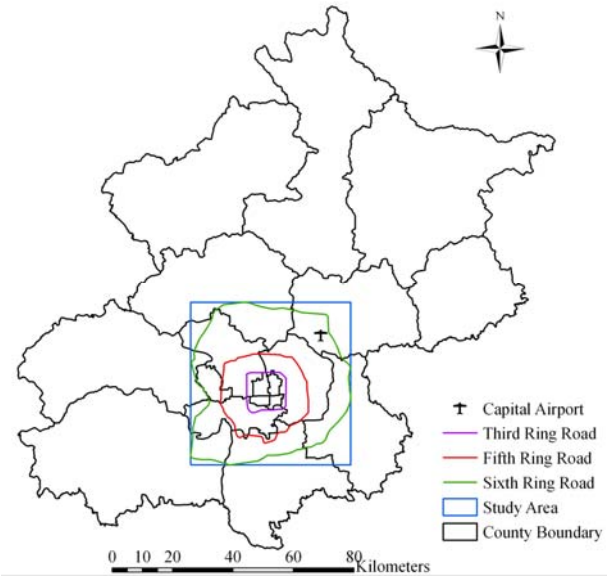

Figure 1. Map of the study area

Two Landsat-5 Thematic Mapper (TM) images, acquired on July 4, 2004 and December 3, 2006, were utilized to examine the spatial distribution of radiation budget in summer and winter in the study area. Both images were geometric rectified with ENVI soft package based on a rectified ASTER VNIR image. Then the digital number (DN) of all bands was

* Corresponding author.

converted into at-sensor spectral radiance following the equation below (Chander & Markham, 2003):

$$L_\lambda = G_{rescale} \times Q_{cal} + B_{rescale} \quad (1)$$

where L_λ=at-sensor spectral radiance in W/(m^2·sr·μm)
$G_{rescale}$, $B_{rescale}$=band-specific rescaling factors
Q_{cal}=quantized calibrated pixel value in DNs.

The Second Simulation of the Satellite Signal in the Solar Spectrum (6S) model was further applied for atmospheric correction of bands 1~5 and 7. For the thermal band, at-sensor brightness temperature was calculated following Chander & Markham (2003):

$$T_B = \frac{K_2}{\ln(K_1 / L_\lambda + 1)} \quad (2)$$

where T_B=at-sensor brightness temperature in K
K_1=607.76W/m^2·sr·μm
K_2=1260.56K

Each image was classified into seven types of land cover: forest, crop, soil, grassland, high-rise building surface, low-rise building surface and water, through the combined method of maximum-likelihood and visual interpretation. Cirrus clouds and their shadows were masked out for the image of July 6, 2004. Random samples were utilized to assess the classification accuracy, it was found that the resultant classification accuracy for the summer and winter images was 83.67% and 86.90%, respectively.

The ground conventional meteorological data including atmospheric temperature and relative humidity used in this study were acquired from observations of the automated weather stations (AWSs) managed by Beijing Meteorological Bureau. In order to account altitude, atmospheric temperature at each station was interpolated following the routine proposed by Kato & Yamaguchi (2005), while the relative humidity was interpolated with the Inverse Distance Weighting (IDW) to the entire study area. The hourly integrated of the total incoming solar radiation (MJ/m^2) (sum of the direct solar radiation and the downward solar diffuse radiation at the ground surface) measured at Beijing Weather Observatory (39°48′N, 116°28′E) was converted to hourly averaged data (W/m^2), which was assumed to be constant throughout the study area because of its limited extent.

3. METHODOLOGY

3.1 Calculation of net radiation

The net radiation flux can be calculated by (Sheng *et al.*, 2003):

$$R_n = R_s(1-\alpha) + \varepsilon\varepsilon_a\sigma T_a^4 - \varepsilon\sigma T_s^4 \quad (3)$$

Where R_n=net radiation at the ground surface in W/m^2
R_s=the total incoming radiation at the ground surface in W/m^2
a=the surface broadband albedo
ε=land surface emissivity
ε_a=atmospheric emissivity
σ=Stefan-Boltzmann constant
T_a=atmospheric temperature near ground surface in K
T_s=land surface temperature in K

3.2 Albedo

According to Liang (2000), the surface broadband albedo can be retrieved based on the spectral albedo for Landsat TM data:

$$\alpha = 0.356\alpha_1 + 0.130\alpha_3 + 0.373\alpha_4 + 0.085\alpha_5 + 0.072\alpha_7 - 0.0018 \quad (4)$$

where α_i=surface reflectance in band i for Landsat TM data

3.3 Land surface emissivity

In this study, the land surface emissivity was estimated following the NDVI Thresholds Method (NDVI^{THM}) proposed by Sobrino *et al.* (2001). The readers are encouraged to refer to Sobrino *et al.* (2004) and Stathopoulou *et al*. (2007).

3.4 Land surface temperature (LST)

Land surface temperature is one of the most important parameters in land surface processes. Qin *et al.* (2001) proposed a mono-window algorithm for estimating land surface temperature:

$$T_s = [a(1-C-D) + (b(1-C-D)+C+D)T_B - DT_a]/C \quad (5)$$

$$C = \varepsilon\tau \quad (6)$$

$$D = (1-\tau)[1+(1-\varepsilon)\tau] \quad (7)$$

where a=-67.355351
b=0.458606
τ=the total atmospheric transmissivity of the thermal band

4. RESULTS

4.1 Validation of the net radiation flux

The hourly integrated net radiation fluxes measured at Beijing Weather Observatory between 10:00am and 11:00am of local time at these two dates were converted to hourly averaged data (W/m^2) and were used to validate the accuracy of the estimated net radiation fluxes. The result is displayed in Table 1. It can be concluded that the estimation of the net radiation flux reached high accuracy.

Date	Hourly averaged R_n (W/m^2)	Estimated R_n (W/m^2)	Absolute error (W/m^2)	Relative error (%)
2004-7-6	619.44	576.4	-43.08	-6.955
2006-12-3	144.44	162.1	17.63	12.21

Table 1. Comparisons of in situ measured and estimated net radiation (R_n)

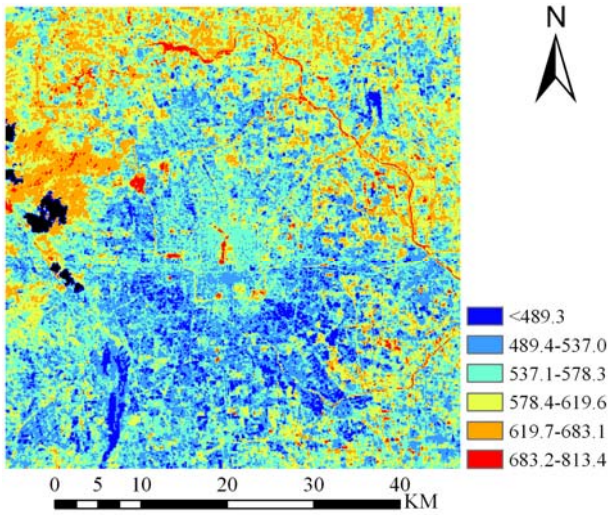

Figure 2. Net radiation (Unit: W/m^2) on July 6, 2004. The black patches denote the masked-out clouds and their shadows.

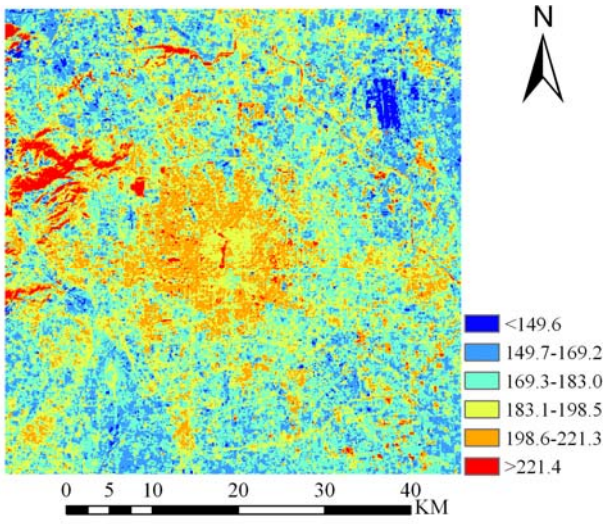

Figure 3. Net radiation (Unit: W/m^2) on December 3, 2006

4.2 Spatial patterns of net radiation

Fig.2 indicates that urban area of the Beijing was a "basin" of the net radiation in the summer. The net radiation exhibited a complicated spatial distribution pattern, which obtained a concentric structure. The net radiation flux was about 537.1~578.3 W/m^2 within the Third Ring Road. While in the south part of the city, the net radiation was mostly less than 537.0 W/m^2 from the Third Ring Road to the Sixth Ring Road, the north part of the city and the hilly areas located in the northwest part had higher net radiation, about 578.4~683.1 W/m^2. Water bodies observed net radiation flux higher than 683.2 W/m^2.

The mean of the net radiation, albedo and land surface temperature were calculated by land cover type, while emissivity was not considered because of its limited variation range over the entire study area. Fig.4, Fig.5 and Fig.6 describe the three parameters of each land cover type. Different land cover types exhibited different radiation budgets, albedo and temperature. Darker and colder surfaces including water and forest absorbed more net radiation, while soil and high-rise types absorbed less because they obtain highest albedo and temperature. The comparison of land surface temperature between urban surface and other natural surfaces indicates that there was intense urban heat island (UHI) effect in the summer in Beijing.

Contrast with the summer, the urban area transferred to a "plateau" of net radiation flux (Fig.3). The concentric pattern was also clearly seen in the distribution map of net radiation flux of the winter. The region within the Fourth Ring Road had a medium value of net radiation, about 183.03~221.29 W/m^2. The net radiation of the regions located beyond the Fourth Ring Road decreased to lower than 183.02 W/m^2. Reservoirs, lakes and hilly areas absorbed the most amount of net radiation, while the Capital Airport received the least. Comparisons between the net radiation flux, albedo and land surface temperature indicate that the radiation flux obtained nearly the same spatial patters as albedo, while was reverse to land surface temperature. Land surface emissivity exhibited less influence on the spatial pattern of the net radiation flux.

Statistics to each land cover type explains the spatial distribution pattern of net radiation in the winter. Soil, as the main body of the suburban areas, exhibited brighter and hotter than other surfaces. On the other hand, urban surface absorbed more net radiation than soil, because of their lower albedo and temperature. Comparisons show that there was slight urban cool island (UCL) effect in the winter in Beijing. This is according with Wang *et al.* (2007).

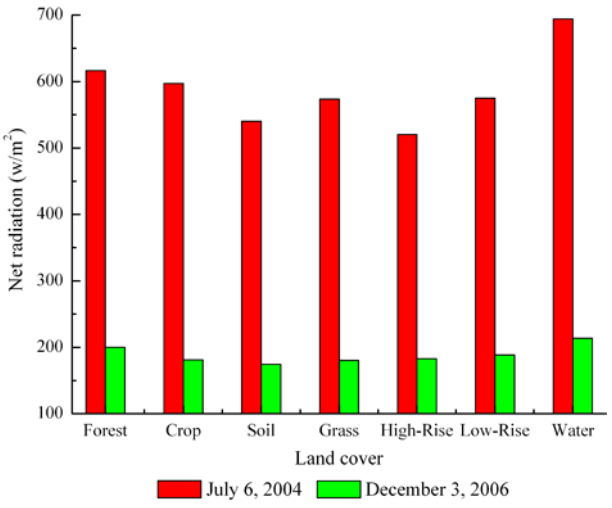

Figure 4. Statistics of net radiation flux on July 6, 2004 and December 3, 2006

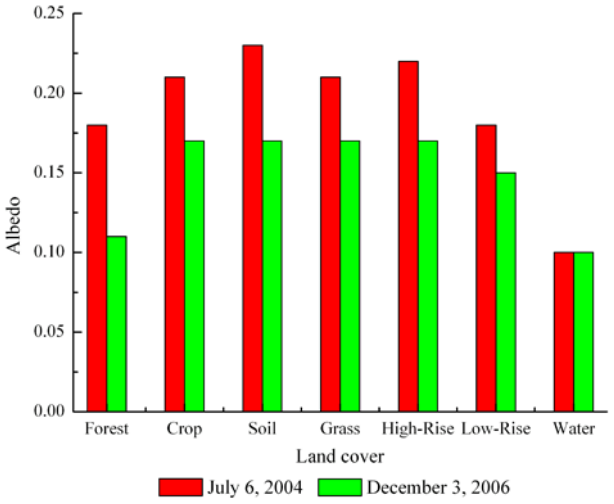

Figure 5. Statistics of albedo on July 6, 2004 and December 3, 2006

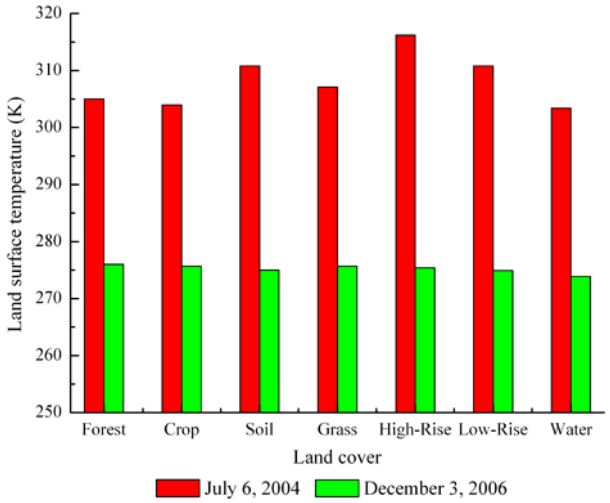

Figure 6. Statistics of land surface temperature on July 6, 2004 and December 3, 2006

4.3 Seasonal change in net radiation

As a primary parameter in land surface processes, the seasonal variation of albedo was an important factor for causing the difference in the radiation budgets. From summer to winter, there were prominent decreases in albedo over all surfaces. While water decreased about 4.14%, other surfaces reduced by 18.40%~36.47%. Decrease of albedo enhanced the ability to absorb the total incoming radiation. On the other hand, the amount of the incoming irradiance reaching the ground decreased dramatically in the winter, which was determined by solar elevation angle (SEA). When Landsat-5 passed on July 6, 2004, SEA was 62.96°, and the measured total incoming radiation was 872.22W/m^2; while SEA decreased to 25.79° and the incoming radiation to 375.00 W/m^2 on December 3, 2006. It can be concluded that the changes in albedo and solar irradiance led to the change in radiation budgets, but the latter played a more important role.

Longwave emission is controlled by land surface temperature. In the winter, because the energy absorbed by land surfaces decreased significantly, land surface temperature decreased accordingly. The longwave emission in the winter was only about 33.22%~ 40.76% of that in the summer. However, the different between the shortwave net radiation flux and the longwave emission decrease largely in winter compared with that in summer. It should be noted that, the heat island and cool land caused by the thermal inertia (Wang *et al.*, 2007), play an importance role in the spatial patterns of net radiation fluxes in summer and winter. As a result, the city turned into a "plateau" in the net radiation map of the winter from a "basin" of the summer.

5. CONCLUSTIONS

It is important to investigate the radiation budgets over urban and suburban surfaces for urban climate research. In this paper, the applicability and feasibility of Landsat-5 TM images in conjunction with meteorological data were investigated to estimate the radiation budgets in Beijing, China. Validation using *in situ* measurements suggests that the estimation accuracy for the net radiation was acceptable. It is concluded that satellite remote sensing can be used as an effective technique to improve modeling and analysis of the spatial patterns of surface energy balance for a mega-city such as Beijing.

It is found that the net radiation in Beijing has unique features with spatial distribution. In the summer, urban area was the "basin" in the distribution map of the net radiation flux, while transferred to the "plateau" in the winter. Concentric patterns can be seen in the map of the radiation flux in both the summer and the winter. This interesting phenomenon can be explained by the distribution of albedo and land surface temperature in urban and suburban areas. The seasonal variations of radiation budgets were also investigated. From summer to winter, the decrease in the shortwave net radiation and the net radiation were mainly controlled by the change in solar elevation angle.

REFERENCES

Bisht, G., Venturini, V., Islam, S., et al., 2005. Estimation of the net radiation using MODIS (Moderate Resolution Imaging Spectroradiometer) data for clear sky days. *Remote Sensing of Environment*, 97, pp. 52-67.

Chander, G., Markham, B., 2003. Revised Landsat-5 TM radiometric calibration procedures and postcalibration dynamic ranges. *IEEE Transactions on Geoscience and Remote Sensing,* 41, pp. 2674-2677.

Chrysoulakis, N., 2003. Estimation of the all-wave urban surface radiation balance by use of ASTER multispectral imagery and in situ spatial data. *Journal of Geophysical Research*, 108, 4582, doi: 10.1029/2003JD003396.

Frey, C., Rigo, G., Parlow, E., 2007. Urban radiation balance of two coastal cities in a hot and dry environment. *International Journal of Remote Sensing*, 28, pp. 2695-2712.

Kato, S., Yamaguchi, Y., 2005. Analysis of urban heat-island effect using ASTER and ETM+ data: separation of anthropogenic heat discharge and natural heat radiation from sensible heat flux. *Remote Sensing of Environment*, 99, pp. 44-54.

Liang, S., 2000. Narrowband to broadband conversions of land surface albedo I algorithmes. *Remote Sensing of Environment*, 76, pp. 213-238.

Qin, Z., Karnieli, A., Berliner, P., 2001. A mono-window algorithm for retrieving land surface temperature from Landsat TM data and its application to the Israel-Egypt border region. *International Journal of Remote Sensing*, 22, pp. 3719-3746.

Rigo, G., Parlow, E., 2007. Modelling the ground heat flux of an urban area using remote sensing data. *Theoretical and Applied Climatology*, doi: 10.1007/s00704-006-0279-8.

Sobrino, J., Raissouni, N., Li, Z., 2001. A comparative study of land surface emissivity retrieval from NOAA data. *Remote Sensing of Environment*, 75, pp. 256-266.

Sobrino, J., Jiménez-Muñoz, J., Paolini, L., 2004. Land surface temperature retrieval from Landsat TM 5. *Remote Sensing of Environment*, 90, pp. 434-440.

Stathopoulou, M., Cartalis, C., Petrakis, M., 2007. Integrating Corine Land Cover data and Landsat TM for surface emissivity definition: application to the urban area of Athens, Greece. *International Journal of Remote Sensing*, 28, pp. 3291-3304.

Wang, K., Wang, J., Wang, P., et al., 2007. Influences of urbanization on surface characteristics as derived from the Moderate-Resolution Imaging Spectroradiometer: A case study for the Beijing metropolitan area. *Journal of Geophysical Research*, 112, D22S06, doi: 10.1029/2006JD007997.

Sheng, P., Mao, J., Li, J., et al., 2003. *Atmospheric Physics*. Peking University Press, Beijing, pp. 107-115.

ACKNOWLEDGEMENTS

This work is supported by National Natural Science Foundation of China (40771136, 40701114), Open Fund of State Key Laboratory of Remote Sensing Science, Jointly Sponsored by Beijing Normal University and the Institute of Remote Sensing Applications of Chinese Academy of Sciences, and National 973 Project (2007CB714403) of China.